Dalton Transactions

ROYAL SOCIETY OF CHEMISTRY

PAPER

View Article Online
View Journal | View Issue

Check for updates

Cite this: *Dalton Trans.*, 2024, **53**, 11952

Received 12th June 2024,
Accepted 27th June 2024

DOI: 10.1039/d4dt01402b

rsc.li/dalton

Synthesis and reactivity of N-heterocyclic carbene (NHC) gold-fluoroalkoxide complexes†

Pierre Arnaut,[a] Nestor Bracho Pozsoni,[a] Fady Nahra,[a,b] Nikolaos V. Tzouras[a]* and Steven P. Nolan[a]*

We disclose a novel series of N-heterocyclic carbene (NHC) gold complexes with varied steric and electronic properties, bearing fluorinated alkoxide anions. Early reactivity studies involving these synthons, lead to the synthesis of various complexes of relevance to gold chemistry and catalysis.

Introduction

It is now well established that fluorinated alcohols are powerful tools in organic chemistry that combine high polarity, low nucleophilicity, and strong hydrogen-bond donor character.[1,2] The presence of electron-withdrawing fluoroalkyl groups grant the alcohols unique solvating properties through hydrogen bonding networks.[3,4] These can be especially useful as solvents in heterocycle synthesis,[5,6] C–H functionalization,[7] cross-coupling reactions,[8,9] and in the controlled deprotection of functional groups in the presence of other labile protected groups.[10] It is worth mentioning that among these, a specific member of this family of alcohols, hexafluoroisopropanol, (HFIP) has been deployed in numerous applications in the chemistry of peptides, as this last deprotection strategy is a key step in the total synthesis of human insulin (on *N*-trityl and *N*-Bpoc groups).[11]

Compared to other fluorinated alcohols such as trifluoroethanol (TFE), HFIP possesses a lower boiling point and a higher melting point, making it a particularly attractive solvent since it can be easily recycled without preventing its use in synthesis at moderate temperatures (below 60 °C). HFIP can promote reactivity in three major ways: it can increase acidity through hydrogen bonding clusters, provide electrostatic stabilization of ionic species, and assist in ionization through coordination.[12] The effects of hydrogen bonding are especially valuable in catalysis, whether it is for electrophile or catalyst activation.[13,14] In gold catalysis, gold–chloride complexes require the use of additives such as silver or potassium salts to be rendered active.[15,16] Indeed, it is only through halogen abstraction that the highly electrophilic gold cationic species is generated.[17] HFIP has recently been used for this purpose and is able, through hydrogen bonding, to weaken the gold–chloride bond.[18] The two most noticeable advantages of [AuCl(NHC)] complexes are their stability and ease of synthesis *via* the weak base route,[14] which is now routinely deployed for a plethora of gold-NHC complexes.[19–21] In comparison, gold-alkoxide complexes have been shown to be very unstable in solution and can be easily converted to their hydroxide equivalent when placed in contact with water.[22] As for the NHC gold hydroxides themselves, the use of strong bases remains unavoidable at this time for their synthesis.[19,22,23]

The chemistry of gold complexes has been the subject of intense research over the past decades.[24,25] The earlier examples of gold-fluoroalkoxide species from Komiya and coworkers permitted the condensation of benzaldehyde as well as the ring opening of thiiranes with gold–phosphine complexes.[26,27] The ability of these complexes to abstract protons from a wide range of substrates is the driving force behind their reactivity, to generate the corresponding carbonyl organogold compounds.[28,29] The incorporation of NHC ligands later led to the isolation of the first gold-hydroxide complex,[30] which was then engaged in the carboxylation of oxazole through C–H activation, among many other synthetic and catalytic applications.[31] More recently, the role of gold-phenoxides in the hydrophenoxylation of alkynes has been described for both mono[32] and dual activation.[33] NHC gold-aryloxides can be also synthesized from NHC gold–chloride and enable the hydration of phenylacetylene.[34] Yet despite these remarkable advances, the synthesis and reactivity of NHC gold-polyfluoroalkoxide complexes has remained underexplored. Therefore, we investigated such systems to seek potential benefits of gold-fluoroalkoxide species from a practical perspective.

[a]*Department of Chemistry and Centre for Sustainable Chemistry, Ghent University, Krijgslaan 281, S-3, 9000 Ghent, Belgium. E-mail: nikolaos.tzouras@ugent.be, steven.nolan@ugent.be*
[b]*Materials & Chemistry (MATCH) unit, VITO (Flemish Institute for Technological Research), Boeretang 200, 2400 Mol, Belgium*

†Electronic supplementary information (ESI) available. CCDC 2311517. For ESI and crystallographic data in CIF or other electronic format see DOI: https://doi.org/10.1039/d4dt01402b

Results and discussion

Our study begins with the use of a standard NHC ligand, *N*,*N*′-bis(2,6-diisopropylphenyl)imidazol-2-ylidene (IPr) bound to gold. As we have previously disclosed,[14] [Au(IPr)(OCH(CF$_3$)$_2$)] (**1a**) can be generated at room temperature from [Au(IPr)(OH)] in benzene within one hour. An even more straightforward route makes use of [Au(IPr)Cl] and 3 equivalents (eq.) of K_2CO_3, stirred at room temperature in dry ethanol for thirty minutes with 1.1 eq. of HFIP. This weak base route can also be performed on a gram-scale in high yields (see, Experimental section). It should be noted that no reaction is observed in the absence of base. Additionally, alternate bases such as NEt_3 and NaOAc proved to be inactive in leading to the desired product. To explore the efficacy of the weak base route on other fluorinated alcohols, the use of trifluoroethanol (TFE) was examined overnight under the same conditions and led to the formation of **2a** (eqn (1)) in high yield.

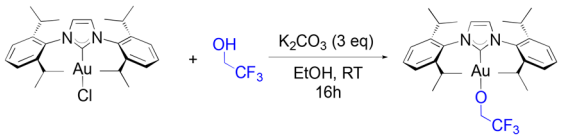

2a (95%) (1)

Several [Au(NHC)] core structures were subjected to this simple protocol and results are presented in Scheme 1. Changing the backbone from electron withdrawing to electron donating groups with IPr^{Cl} (**1c**) and IPr^{Me} (**1d**) had no negative impact on isolated yields, but SIPr (**1b**) could only be isolated with 75% isolated yield. Increasing the bulk of the ligand from IPr to IPr* (**1f**) did not noticeably affect the yield. The molecular structure of **1d** is presented in Fig. 1 with a selection of bond distances and angles. In the extreme case of the exceedingly bulky IPr$^{\#}$ however, steric effects drastically hindered reactivity, and no improvement was made even when other solvents, such as THF, were used. As for *N*-alkyl-bearing ligands, the I^{t}Bu complex **1h** was obtained with 98% yield. The fluoroalkoxide complex can also be accessed in high yield through this method when a tertiary phosphine ligand is used (**1j**).

Boronic acids were initially tested in our reactivity study for the arylation of the gold-fluoroalkoxide complexes. When **1a** was reacted with phenyl, 2-naphthyl, 4-fluorophenyl and 4-trifluoromethylphenyl boronic acids, the desired gold-aryl derivatives (**3a**, **3b**, **3c** and **3d**, respectively) were obtained in excellent yields in reaction times of two hours at room temperature (Scheme 2).

To our knowledge, short reaction times for these transformations had only been achieved thus far by relying on the use of strong bases such as KOH on the gold hydroxide.[35] Following the weak base route from [Au(IPr)Cl], the synthesis of these same products requires between 4 to 24 hours.[36,37] However, no desired product was observed from the reaction of **1a** with 4-methoxyphenyl boronic acid, and the same result was observed on 4-tolyl boronic acid. Finally, under identical conditions to HFIP, TFE gave a noticeably lower, but still acceptable yield with phenylboronic acid (eqn (2)).

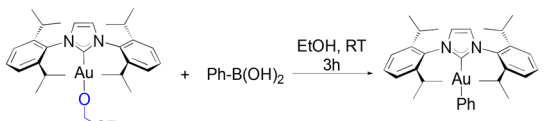

2a **3a** (76%) (2)

Alkynyl complexes can be easily accessed from [Au(IPr)Cl], 2 eq. of phenylacetylene and 3 eq. of sodium acetate in

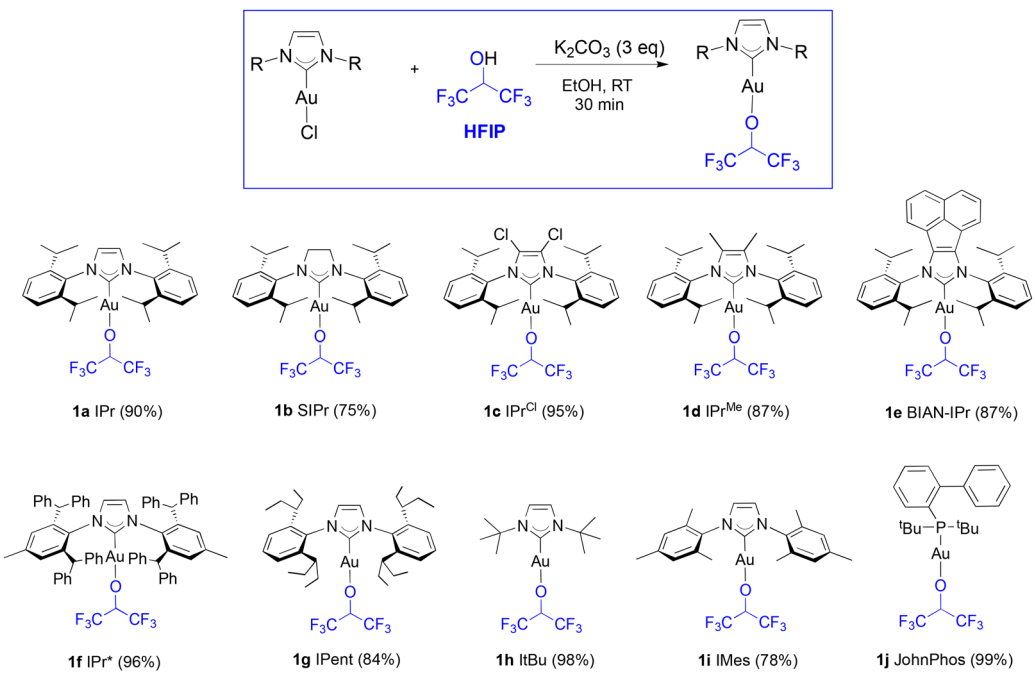

Scheme 1 Synthetic route to various NHC and phosphine bearing gold-fluoroalkoxide complexes.

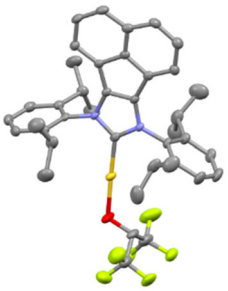

Fig. 1 X-ray molecular structure of **1e** showing thermal displacement ellipsoids at the 50% probability level. Hydrogen atoms omitted for clarity. Selected bond distances (Å) and angles (deg): Au–O 2.017(1), Au–C 1.948(1); O–C_{HFIP} 1.372(1); N–C–N 106.29, C_{NHC}–Au–O 175.89 (13). CCDC 2311517.†

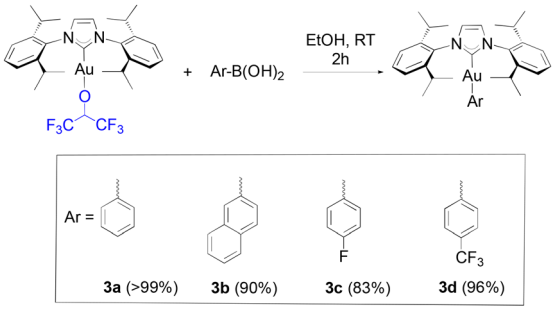

Scheme 2 Scope of boronic acids synthesized in this study with isolated yields given in parentheses.

ethanol at room temperature yielding the product in a 93% yield.[38] When **1a** was used as the starting gold synthon, a 75% yield was reached under the same conditions. Improved results were achieved at higher temperatures (60 °C) with a 94% yield obtained of **4a** after one hour (Scheme 3).

The lower reactivity of **1a** compared to that displayed by [Au(IPr)(OH)] is overcome by using a slightly higher reaction temperature. The same is observed when **1i** reacts with phenylacetylene to yield **4b**, in one hour. When using **1f**, only a 50% conversion is observed within the first hour (or up to 80% with 3 eq. of alkyne) in the alkynylation reaction. The slower kinetics must be caused by the significant higher steric hindrance of the bulky IPr* compared to that of IPr. Nevertheless, high yields can still be obtained for **4c** after three hours, and further improved to 85% with the use of an excess of the alkyne (3 eq.).

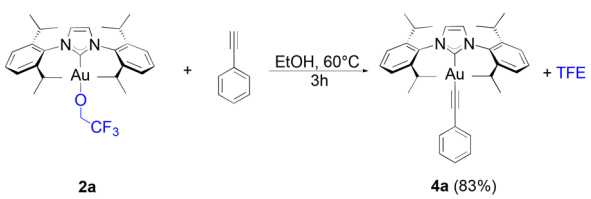

(3)

Using **2a** as the starting gold complex requires slightly longer reaction times than when **1a** is used and full conversion is not observed after 60 minutes (eqn (3)). This is surprising as

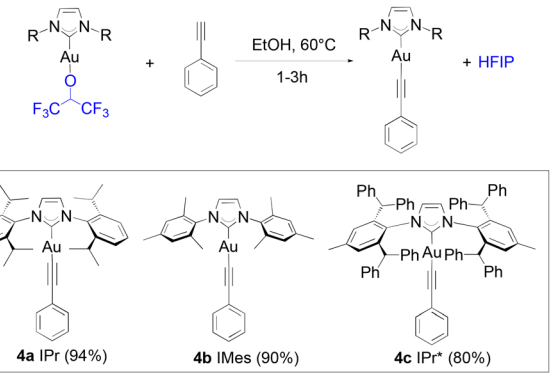

Scheme 3 Scope and reaction conditions for the synthesis of gold-acetylide complexes.

TFE, being more electron rich than HFIP, would be expected to be more reactive. Considering that HFIP has a lower boiling point than TFE (58 °C compared to 74 °C), the evaporation of HFIP during the reaction might be the reason behind the shift in equilibrium in favour of the gold-alkynyl bond formation.

Another example of the reactivity of **1a** is exemplified with a carbazole substrate resulting in the formation of complex **5** in a 96% yield in ethanol within one hour, but did require heating at 60 °C, whereas the weak base route can be performed at room temperature but requires a 24-hour reaction time. It should be noted that this gold complex **5** appears extremely versatile as a photocatalyst in cycloaddition reactions (Scheme 4).[38–41]

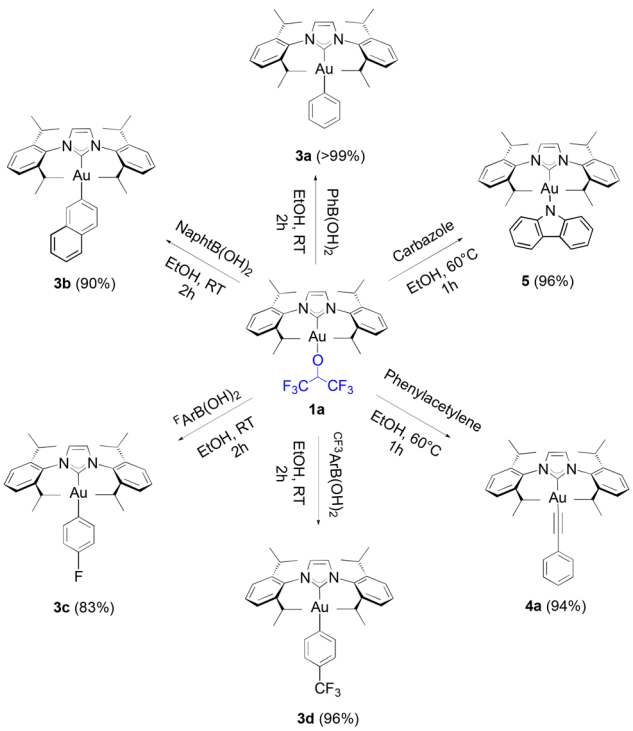

Scheme 4 Examples of the use of **1a** as synthon.

To confirm the catalytic efficacy of our well-defined [Au(NHC)(OCH(CF$_3$)$_2$)] complexes, **1a** was deployed in the addition of carboxylic acids to alkynes (eqn (4)) resulting in an 80% yield. This compares to NMR yields of 87% using the [Au(IPr)(cbz)] (cbz = carbazolyl) catalyst under identical conditions.[42]

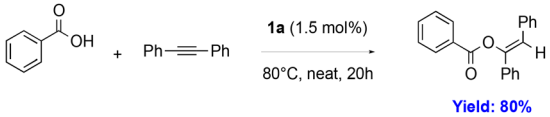

(4)

The weak base route is routinely used in the synthesis of [Au(NHC)Cl] complexes and now enables access to a variety of bench-stable gold fluoroalkoxide complexes. These fluoroalkoxide complexes display C$_{sp}$–H/N–H bond activation properties and permit the synthesis of aryl-, alkynyl- and amido gold complexes. A remarkable feature of the gold-fluoroalkoxides is their generally high solubility which also extends to non-polar organic solvents, such as benzene and toluene. In the context of organometallic synthesis, this feature can be advantageous, especially along with their stability and ease of access. Therefore, these complexes possess valuable properties that are complementary to those of the gold hydroxides, even though the latter display higher and wider reactivity. The presence of stable gold-alkoxide moieties will make these well-defined and easily synthesized complexes invaluable synthetic and mechanistic probes that will permit further advances in gold chemistry and catalysis.

Experimental synthetic procedures

Synthesis of 1a

[Au(IPr)Cl] (200 mg, 0.32 mmol) is charged in a 4 mL vial and suspended in 1 mL of ethanol with 37 μL of HFIP (0.35 mmol, 1.1 eq.) in the presence of K_2CO_3 (134 mg, 0.96 mmol, 3 eq.). The reaction is left at room temperature under magnetic stirring overnight for 30 minutes. After this time, the solvent is evaporated, the residue is microfiltered with 8 mL of toluene and filtered through basic alumina. The solution is then concentrated on the rotary evaporator until it becomes a viscous oil. The product is triturated with pentane (5 mL) and isolated as a microcrystalline white solid upon decantation and drying under vacuum in 90% yield (220 mg). Spectroscopic data match those found in the literature.[14]

Gram-scale synthesis of 1a

Identical protocol as above starting from [Au(IPr)Cl] (1.00 g, 1.61 mmol) and K_2CO_3 (667 mg, 4.83 mmol, 3 eq.) in a 10 mL vial with 5 mL of ethanol and 339 μL of HFIP (3.22 mmol, 2 eq.). **1a** is thus obtained as a microcrystalline solid in a 93% yield (1.13 g).

^{1}H NMR (300 MHz, $CDCl_3$) δ 7.53–7.47 (t, J = 7.7 Hz, 2H), 7.29 (d, J = 7.8 Hz, 4H), 7.17 (s, 2H), 4.23 (hept, J = 6.4 Hz, 1H), 2.53 (hept, J = 6.9 Hz, 4H), 1.32 (d, J = 6.9 Hz, 12H), 1.21 (d, J = 6.9 Hz, 12H).

Synthesis of 1b

Identical protocol as **1a** starting from [Au(SIPr)Cl] (100 mg, 0.16 mmol) and K_2CO_3 (66 mg, 0.48 mmol, 3 eq.) with 1 mL of ethanol and 18 μL of HFIP (0.17 mmol, 1.1 eq.). **1b** is thus obtained as a microcrystalline solid in a 75% yield (92 mg).

^{1}H NMR (300 MHz, $CDCl_3$) δ 7.41 (t, J = 7.7 Hz, 2H), 7.25 (d, J = 5.4 Hz, 4H), 7.22 (s, 2H), 4.17–4.08 (m, 1H), 4.05 (s, 4H), 3.02 (hept, J = 6.9 Hz, 4H), 1.40 (d, J = 6.8 Hz, 12H), 1.33 (d, J = 6.9 Hz, 12H).

^{13}C NMR (100 MHz, $CDCl_3$) δ 189.41 (Au–C), 146.3 (C_{Ar}), 133.9 (CH_{Ar}), 129.7 (C_{Ar}), 124.3 (CH_{Ar}), 76.2 (p, J_{CF} = 30.3 Hz, $CH(CF_3)$), 53.1 (NC_{imid}), 28.7 ($CH(CH_3)_2$), 24.4 ($CH(CH_3)_2$), 24.1 ($CH(CH_3)_2$).

^{19}F NMR (500 MHz, $CDCl_3$) δ −76.59 (s, CF_3).

HRMS (ESI): m/z [M + CH_3CN] calcd for $C_{29}H_{41}AuN_3$: 628.2966. Found: 628.2952.

Synthesis of 1c

Same protocol as **1a** from [Au(IPr^{Cl})Cl] (50 mg, 0.07 mmol) and K_2CO_3 (30 mg, 0.21 mmol, 3 eq.) with 0.5 mL of ethanol and 8 μL of HFIP (0.07 mmol, 1.1 eq.). **1c** is thus obtained as a microcrystalline solid in a 95% yield (56 mg).

^{1}H NMR (300 MHz, $CDCl_3$) δ 7.55 (td, J = 7.8, 1.9 Hz, 2H), 7.32 (d, J = 7.8 Hz, 4H), 4.20 (p, J = 6.3 Hz, 1H), 2.45 (h, J = 6.9 Hz, 4H), 1.33 (dd, J = 6.8, 1.6 Hz, 12H), 1.25 (d, J = 6.9 Hz, 12H).

^{13}C NMR (100 MHz, $CDCl_3$) δ 167.7 (Au–C), 146.1 (C_{Ar}), 131.6 (CH_{Ar}), 131.5 (C_{Ar}), 124.6 (CH_{Ar}), 118.8 (NC_{imid}), 77.1 (p, J_{CF} = 30.5 Hz, $CH(CF_3)$), 29.2 ($CH(CH_3)_2$), 24.2 ($CH(CH_3)_2$), 23.7 ($CH(CH_3)_2$).

^{19}F NMR (500 MHz, $CDCl_3$) δ −76.48 (s, CF_3).

HRMS (ESI): m/z [M + CH_3CN] calcd for $C_{29}H_{37}AuCl_2N_3$: 694.2030. Found: 694.2013.

Synthesis of 1d

Same protocol as **1a** starting from [Au(IPr^{Me})Cl] (100 mg, 0.15 mmol) and K_2CO_3 (63 mg, 0.46 mmol, 3 eq.) with 1 mL of ethanol and 17 μL of HFIP (0.16 mmol, 1.1 eq.). **1d** is thus obtained as a microcrystalline solid in a 87% yield (104 mg).

^{1}H NMR (300 MHz, $CDCl_3$) 7.48 (td, J = 7.8, 2.1 Hz, 2H), 7.28 (d, J = 7.3 Hz, 4H), 4.19 (hept, J = 6.4 Hz, 1H), 2.43 (tt, J = 13.9, 6.9 Hz, 4H), 1.94 (d, J = 6.1 Hz, 6H), 1.33 (d, 12H), 1.22 (d, 12H).

^{13}C NMR (100 MHz, $CDCl_3$) δ 163.8 (Au–C), 145.9 (C_{Ar}), 132.6 (C_{Ar}), 130.5 (CH_{Ar}), 126.1 (CH_{Ar}), 124.4 (NC_{imid}), 76.9 (p, J_{CF} = 29.9 Hz, $CH(CF_3)$), 28.8 ($CH(CH_3)_2$), 25.2 ($CH(CH_3)_2$), 24.7 ($CH(CH_3)_2$), 23.6 (CH_3), 23.5 (CH_3).

^{19}F NMR (500 MHz, $CDCl_3$) δ −76.41 (s, CF_3).

HRMS (ESI): m/z [M + CH_3CN] calcd for $C_{31}H_{43}AuN_3$: 654.3123. Found: 654.3104.

Synthesis of 1e

Identical protocol as **1a** starting from [Au(BIAN-IPr)Cl] (100 mg, 0.13 mmol) and K_2CO_3 (55 mg, 0.40 mmol, 3 eq.) with 1 mL of ethanol and 16 μL of HFIP (0.14 mmol, 1.1 eq.). **1e** is thus obtained as a microcrystalline solid in a 87% yield (102 mg). Crystals suitable for single crystal X-ray diffraction were grown *via* vapor diffusion of hexane into a saturated solution of the product in benzene.

^{1}H NMR (300 MHz, C_6D_6) δ 7.32 (dd, J = 8.4, 7.2 Hz, 2H), 7.23 (dd, J = 8.1, 1.0 Hz, 4H), 6.87 (d, J = 7.0 Hz, 2H), 6.82 (t, J = 7.2 Hz, 2H), 6.79 (d, J = 6.4 Hz, 2H), 4.78 (p, J = 6.4 Hz, 1H),

2.94 (hept, J = 6.7 Hz, 4H), 1.45 (d, J = 6.9 Hz, 12H), 0.96 (d, J = 6.9 Hz, 12H).

^{1}H NMR (300 MHz, $CDCl_3$) δ 7.66 (d, J = 8.3 Hz, 2H), 7.49–7.42 (t, J = 7.8 Hz, 2H), 7.32–7.26 (m, 2H), 7.26 (d, J = 7.8 Hz, 4H), 7.11 (s, 1H), 6.88 (d, J = 7.0 Hz, 2H), 4.14 (p, J = 6.4 Hz, 1H), 2.66 (hept, J = 6.7 Hz, 4H), 1.22 (d, J = 6.9 Hz, 12H), 0.95 (d, J = 6.9 Hz, 12H).

^{13}C NMR (100 MHz, $CDCl_3$) δ 172.4 (Au–C), 145.7 (C_{Ar}), 138.1 (C_{Ar}), 133.0 (C_{BIAN}), 130.9 (CH_{Ar}), 129.9 (C_{BIAN}), 128.6 (CH_{BIAN}), 127.9 (CH_{BIAN}), 125.5 (C_{BIAN}), 124.6 (CH_{Ar}), 121.3 (C_{BIAN}), 76.9 (p, J_{CF} = 30.0 Hz, $CH(CF_3)$), 29.1 ($CH(CH_3)_2$), 24.2 ($CH(CH_3)_2$), 24.1 ($CH(CH_3)_2$).

^{19}F NMR (500 MHz, $CDCl_3$) δ −76.35 (s, CF_3).

Synthesis of 1f

Same protocol as **1a** starting from [Au(IPr*)Cl] (100 mg, 0.08 mmol) and K_2CO_3 (36 mg, 0.26 mmol, 3 eq.) with 1 mL of ethanol and 10 μL of HFIP (0.09 mmol, 1.1 eq.). **1f** is thus obtained as a microcrystalline solid in a 96% yield (107 mg).

^{1}H NMR (300 MHz, $CDCl_3$) δ 7.22–7.11 (m, 32H), 6.86–6.82 (m, 12H), 5.65 (s, 2H), 5.30 (s, 4H), 4.32 (p, J = 6.3 Hz, 1H), 2.24 (s, 6H).

^{13}C NMR (100 MHz, $CDCl_3$) δ 167.6 (Au–C), 143.0 (C_{Ar}), 142.6 (C_{Ar}), 141.0 (C_{Ar}), 140.2 (C_{Ar}), 133.8 (CH_{Ar}), 130.2 (CH_{Ar}), 129.8 (CH_{Ar}), 129.4 (CH_{Ar}), 128.6 (CH_{Ar}), 128.4 (CH_{Ar}), 126.8 (CH_{Ar}), 126.7 (CH_{Ar}), 123.2 (NCH_{imid}), 77.2 (p, J_{CF} = 30.2 Hz, $CH(CF_3)_2$), 21.9 (CH_3).

^{19}F NMR (500 MHz, $CDCl_3$) δ −76.23 (s, CF_3).

HRMS (ESI): m/z [M + CH_3CN] calcd for $C_{71}H_{59}AuN_3$: 1150.4375. Found: 1150.4610.

Synthesis of 1g

Same protocol as **1a** starting from [Au(IPent)Cl] (100 mg, 0.16 mmol) and K_2CO_3 (70 mg, 0.50 mmol, 3 eq.) with 1 mL of ethanol and 19 μL of HFIP (0.18 mmol, 1.1 eq.). **1g** is thus obtained as a microcrystalline solid in a 84% yield (59 mg).

^{1}H NMR (300 MHz, $CDCl_3$) δ 7.48 (t, J = 7.8 Hz, 2H), 7.20 (d, J = 7.7 Hz, 4H), 7.03 (s, 2H), 4.15 (hept, J = 6.4 Hz, 1H), 2.15 (p, J = 7.2 Hz, 4H), 1.92–1.58 (m, 12H), 1.55–1.39 (m, 4H), 0.93 (t, J = 7.4 Hz, 12H), 0.78 (t, J = 7.4 Hz, 12H).

^{13}C NMR (100 MHz, $CDCl_3$) δ 167.3 (Au–C), 143.4 (C_{Ar}), 136.8 (CH_{Ar}), 130.2 (C_{Ar}), 124.8 (CH_{Ar}), 123.6 (NC_{imid}), 76.5 (p, J_{CF} = 29.9 Hz, $CH(CF_3)$), 42.9, ($CH(CH_2)_2$), 29.1, ($CH_2(CH_3)_2$) 28.2 ($CH_2(CH_3)_2$), 12.6 (CH_2CH_3).

^{19}F NMR (500 MHz, $CDCl_3$) δ −76.52 (s, CF_3).

HRMS (ESI): m/z [M + CH_3CN] calcd for $C_{37}H_{55}AuN_3$: 738.4062. Found: 738.4043.

Synthesis of 1h

Same protocol as **1a** starting from [Au(I^{t}Bu)Cl] (100 mg, 0.24 mmol) and K_2CO_3 (100 mg, 0.72 mmol, 3 eq.) with 1 mL of ethanol and 28 μL of HFIP (0.26 mmol, 1.1 eq.). **1h** is thus obtained as a microcrystalline solid in a 98% yield (131 mg).

^{1}H NMR (300 MHz, $CDCl_3$) δ 7.06 (s, 2H), 4.77 (hept, J = 6.4 Hz, 1H), 1.86 (s, 18H).

^{13}C NMR (100 MHz, $CDCl_3$) δ 159.7 (Au–C), 116.5 (C_{Ar}), 77.7 (p, J_{CF} = 30.1 Hz, $CH(CF_3)$), 59.0 ($C(CH_3)$), 31.9 (CH_3), 31.6 (CH_3).

^{19}F NMR (500 MHz, $CDCl_3$) δ −75.89 (s, CF_3).

HRMS (ESI): m/z [M + CH_3CN] calcd for $C_{13}H_{23}AuN_3$: 418.1557. Found: 418.1547.

Synthesis of 1i

Same protocol as **1a** starting from [Au(IMes)Cl] (100 mg, 0.18 mmol) and K_2CO_3 (76 mg, 0.55 mmol, 3 eq.) with 1 mL of ethanol and 21 μL of HFIP (0.20 mmol, 1.1 eq.). **1i** is thus obtained as a microcrystalline solid in a 78% yield (97 mg).

^{1}H NMR (300 MHz, $CDCl_3$) δ 7.08 (s, 2H), 6.99 (s, 4H), 4.30 (hept, J = 6.4 Hz, 1H), 2.35 (s, 6H), 2.08 (s, 12H).

^{13}C NMR (300 MHz, $CDCl_3$) δ 165.9 (Au–C), 139.8 (C_{Ar}), 134.9 (C_{Ar}), 134.5 (C_{Ar}), 129.4 (CH_{Ar}), 122.2 (NCH_{imid}), 21.2 (CH_3), 17.7 (CH_3).

^{19}F NMR (500 MHz, $CDCl_3$) δ −76.23 (s, CF_3).

HRMS (ESI): m/z [M] calcd for $C_{42}H_{48}AuN_4$: 805.3544. Found: 805.3520.

Synthesis of 1j

Same protocol as **1a** starting from [Au(JohnPhos)Cl] (100 mg, 0.18 mmol) and K_2CO_3 (78 mg, 0.56 mmol, 3 eq.) with 1 mL of ethanol and 21 μL of HFIP (0.20 mmol, 1.1 eq.). **1j** is thus obtained as a microcrystalline solid in a 99% yield (123 mg).

^{1}H NMR (300 MHz, $CDCl_3$) δ 7.86 (td, J = 7.6, 1.7 Hz, 1H), 7.47 (m, 5H), 7.29 (dd, J = 4.3, 2.1 Hz, 1H), 7.19–7.14 (m, 2H), 4.35 (pd, J = 6.4, 2.8 Hz, 1H), 1.40 (d, J = 15.5 Hz, 9H), 1.35 (d, J = 15.4 Hz, 9H).

^{13}C NMR (100 MHz, $CDCl_3$) 133.6 (d, J = 2.7 Hz), 133.4 (d, J = 3.1 Hz), 133.3 (d, J = 7.8 Hz), 130.6 (d, J = 2.4 Hz), 130.6 (d, J = 2.3 Hz), 129.5, 129.3, 128.8, 128.4, 128.3, 126.8 (d, J = 6.8 Hz), 126.7 (d, J = 7.1 Hz), 76.4 (p, J = 28.6 Hz), 31.0 (d, J = 6.7 Hz), 30.8 (d, J = 6.3 Hz).

^{31}P NMR (300 MHz, $CDCl_3$) δ 54.71 (s, P).

^{19}F NMR (500 MHz, $CDCl_3$) δ −75.58 (s, CF_3).

HRMS (ESI): m/z [M + CH_3CN] calcd for $C_{22}H_{30}AuNP$: 536.1781. Found: 536.1772.

Synthesis of 2a

Same protocol as **1a** starting from [Au(IPr)Cl] (200 mg, 0.32 mmol) and K_2CO_3 (133 mg, 0.96 mmol, 3 eq.) with 1 mL of ethanol and 25 μL of TFE (0.35 mmol, 1.1 eq.). **2** is thus obtained as a microcrystalline solid in a 95% yield (210 mg).

^{1}H NMR (300 MHz, $CDCl_3$) δ 7.52–7.46 (t, J = 7.8 Hz, 2H), 7.28 (d, J = 7.9 Hz, 4H), 7.14 (s, 2H), 3.90 (q, J = 9.3 Hz, 2H), 2.55 (hept, J = 6.9 Hz, 4H), 1.35 (d, J = 6.9, 4.8 Hz, 12H), 1.21 (d, J = 6.9, 1.1 Hz, 12H).

^{13}C NMR (300 MHz, $CDCl_3$) δ 169.4 (Au–C), 145.7 (C_{Ar}), 134.3 (C_{Ar}), 130.6 (CH_{Ar}), 124.2 (CH_{Ar}), 123.0 (NCH_{imid}), 68.9 (q, J = 31.7 Hz, $CH_2(CF_3)$), 28.9 ($CH(CH_3)_2$), 24.3 ($CH(CH_3)_2$), 24.2 ($CH(CH_3)_2$).

^{19}F NMR (500 MHz, $CDCl_3$) δ −77.5 (s, CF_3).

HRMS (ESI): m/z [M + CH_3CN] calcd for $C_{29}H_{39}AuN_3$: 626.2810. Found: 626.2800.

Reactions involving boron reagents

Synthesis of 3a from 1a. 1a (100 mg, 0.13 mmol) and phenylboronic acid (16 mg, 0.13 mmol, 1 eq.) are dissolved in 0.6 mL of ethanol and stirred at room temperature for 2 hours. Upon full conversion, the mixture is diluted in neutralized dichloromethane, passed on a microfilter and dried under vacuum to retrieve the product. **3a** is thus obtained as a microcrystalline solid in a 99% yield (87 mg). Spectroscopic data match those found in the literature.[37]

Synthesis of 3a from 2a. Same protocol as **3a** starting from **2a** (100 mg, 0.14 mmol) and phenylboronic acid (17 mg, 0.14 mmol, 1 eq.) with 0.6 mL of ethanol for 3 hours. **3b** is thus obtained as a microcrystalline solid in 76% yield (74 mg).

^{1}H NMR (300 MHz, $CDCl_3$) δ 7.46 (t, J = 7.8 Hz, 2H), 7.27 (d, J = 6.8 Hz, 4H), 7.14 (s, 2H), 7.09–7.05 (m, 2H), 6.99 (t, 2H), 6.85–6.79 (m, 1H), 2.67 (hept, J = 6.7 Hz, 4H), 1.41 (d, J = 6.9 Hz, 12H), 1.24 (d, J = 6.9 Hz, 12H). Spectroscopic data match those found in the literature.[37]

Synthesis of 3b. Same protocol as for **3a** starting from **1a** (100 mg, 0.13 mmol) and 2-naphthylboronic acid (22 mg, 0.13 mmol, 1 eq.) with 0.6 mL of ethanol. **3b** is thus obtained as a microcrystalline solid in a 90% yield (85 mg).

^{1}H NMR (400 MHz, $CDCl_3$) δ 7.56 (dd, J = 16.2, 8.1, 2H), 7.46 (m, 2H), 7.45 (t, J = 8.1 Hz, 2H), 7.30 (d, J = 7.8 Hz, 4H), 7.22 (m, 1H), 7.16 (s, 2H), 7.18–7.14 (m, 2H), 2.70 (hept, J = 6.9 Hz, 4H), 1.44 (d, J = 6.8 Hz, 12H), 1.26 (d, J = 7.0 Hz, 12H). Spectroscopic data match those found in the literature.[37]

Synthesis of 3c. Same protocol as **3a** starting from **1a** (100 mg, 0.13 mmol) and 4-fluorophenylboronic acid (16 mg, 0.13 mmol, 1 eq.) with 0.6 mL of ethanol. **3c** is thus obtained as a microcrystalline solid in an 83% yield (75 mg).

^{1}H NMR (400 MHz, $CDCl_3$) δ 7.47 (t, J = 7.8 Hz, 2H), 7.28 (d, J = 7.8 Hz, 4H), 7.14 (s, 2H), 7.00 (m, 2H), 6.73 (dd, J = 10.3, 8.2 Hz, 2H), 2.66 (hept, J = 7.0 Hz, 4H), 1.39 (d, J = 6.9 Hz, 12H), 1.24 (d, J = 6.9 Hz, 12H). Spectroscopic data match those found in the literature.[43]

Synthesis of 3d. Same protocol as for **3a** starting from **1a** (100 mg, 0.13 mmol) and 4-(trifluoromethyl) phenylboronic acid (16 mg, 0.13 mmol, 1 eq.) with 0.6 mL of ethanol. **3d** is thus obtained as a microcrystalline solid in a 96% yield (93 mg).[37]

^{1}H NMR (400 MHz, $CDCl_3$) δ 7.48 (t, J = 7.8 Hz, 2H), 7.29 (d, J = 7.8 Hz, 4H), 7.20 (d, J = 7.8 Hz, 2H), 7.16 (s, 2H), 7.14 (d, J = 7.9 Hz, 2H), 2.65 (hept, J = 6.9 Hz, 4H), 1.39 (d, J = 6.8 Hz, 12H), 1.24 (d, J = 6.9 Hz, 12H).

Reactions involving non-boron reagents

Synthesis of 4a from 1a. 1a (100 mg, 0.13 mmol) is charged in 4 mL vial and suspended in 0.5 mL of ethanol with phenylacetylene (14 μL, 0.13 mmol, 1 eq.). The solution is stirred at 60 °C for one hour. Once the reaction is complete, the mixture is diluted in neutralized DCM, passed on a microfilter and dried under vacuum to retrieve the product. **4a** is thus obtained as a microcrystalline solid in a 94% yield (85 mg). Spectroscopic data match those found in the literature.[38]

Synthesis of 4a from 2a. Same protocol as above from **2a** (100 mg, 0.14 mmol) with 0.5 mL of ethanol and phenylacetylene (15 μL, 0.14 mmol, 1 eq.). **4a** is thus obtained as a microcrystalline solid in 83% yield (83 mg).

^{1}H NMR (400 MHz, $CDCl_3$) δ 7.49 (t, J = 7.8 Hz, 2H), 7.29 (m, 2H), 7.29 (d, J = 7.8 Hz, 4H), 7.12 (s, 2H), 7.12–7.06 (m, 2H), 7.06–7.03 (m, 1H), 2.61 (hept, J = 6.8 Hz, 4H), 1.38 (d, J = 6.9 Hz, 12H), 1.21 (d, J = 6.9 Hz, 12H). Spectroscopic data match those found in the literature.[38]

Synthesis of 4b. Same protocol as **4a** starting from **1f** (100 mg, 0.14 mmol) with 0.5 mL of ethanol and phenylacetylene (16 μL, 0.14 mmol, 1 eq.). **4b** is thus obtained as a microcrystalline solid in 90% yield (81 mg).

^{1}H NMR (300 MHz, $CDCl_3$) δ 7.35–7.30 (m, 2H), 7.15–7.06 (m, 3H), 7.05 (s, 2H), 6.99 (s, 4H), 2.34 (s, 12H), 2.12 (s, 12H). Spectroscopic data match those found in the literature.[38]

Synthesis of 4c. Same protocol as for **4a** from **1d** (100 mg, 0.07 mmol) with 0.5 mL of ethanol and phenylacetylene (8 μL, 0.07 mmol, 1 eq.) for 3 hours. **4c** is thus obtained as a microcrystalline solid in 80% yield (75 mg).

^{1}H NMR (300 MHz, $CDCl_3$) δ 7.55–7.51 (m, 2H), 7.25–7.11 (m, 40H), 6.87 (d, J = 2.2 Hz, 3H), 6.85 (d, J = 1.0 Hz, 2H), 6.84–6.83 (m, 4H), 5.70 (s, 2H), 5.37 (s, 4H), 2.22 (s, 6H). Spectroscopic data match those found in the literature.[43]

Synthesis of 5. 1a (100 mg, 0.13 mmol) is dissolved in 0.5 mL of ethanol with 1,2,4-carbazole (22 mg, 0.13 mmol, 1 eq.). The solution is stirred at 60 °C for one hour. The product is diluted in THF, dried under vacuum, washed with diethylether and precipitated with pentane. **5** is thus obtained as a microcrystalline solid in a 96% yield (95 mg).

^{1}H NMR (300 MHz, CD_2Cl_2) δ 7.89 (d, J = 7.7 Hz, 2H), 7.65 (t, J = 7.9 Hz, 2H), 7.44 (d, J = 7.8 Hz, 4H), 7.36 (s, 2H), 7.03 (t, J = 7.6 Hz, 2H), 6.86 (t, J = 7.3 Hz, 2H), 6.73 (d, J = 8.1 Hz, 2H), 2.73 (p, J = 7.1 Hz, 4H), 1.38 (d, J = 6.9 Hz, 12H), 1.29 (d, J = 6.9 Hz, 12H). Spectroscopic data match those found in the literature.[39,41]

Catalytic reaction protocol

Benzoic acid (37.7 mg, 0.3 mmol), diphenylacetylene (50 mg, 0.3 mmol) and **1a** (2.2 mg, 1.5 mol%) are stirred neat at 80 °C for 20 hours. After this time, the mixture is microfiltered with diethyl ether (1 mL) and concentrated under vacuum. The product, (*Z*)-1,2-diphenylvinyl benzoate, is triturated with pentane (5 mL) and isolated as a microcrystalline white solid with 80% yield (70 mg). Spectroscopic data match those found in the literature.[42]

^{1}H NMR (300 MHz, $CDCl_3$) δ (ppm) = 8.25 (dd, J = 8.4, 1.4 Hz, 2H, CH_{Ar}), 7.71–7.64 (m, 1H, CH_{Ar}), 7.63–7.51 (m, 6H, CH_{Ar}), 7.41–7.32 (m, 4H, CH_{Ar}), 7.23–7.20 (m, 1H, CH_{Ar}), 6.81 (s, 1H, C═CH).

Conflicts of interest

There are no conflicts to declare.

Acknowledgements

We gratefully thank the Research Foundation – Flanders (FWO) and the Special Research Fund (BOF) of Ghent University (starting and senior grants to S.P.N.). Umicore AG is gratefully thanked for gifts of materials.

References

1 X. An and J. Xiao, *Chem. Rec.*, 2020, **20**, 142–161.
2 P. Trillo, A. Baeza and C. Nájera, *J. Org. Chem.*, 2012, **77**, 7344–7354.
3 F.-X. Tian and J. Qu, *J. Org. Chem.*, 2022, **87**, 1814–1829.
4 X. Zeng, S. Liu, Z. Shi and B. Xu, *Org. Lett.*, 2016, **18**, 4770–4773.
5 S. Khaksar, *J. Fluor. Chem.*, 2015, **172**, 51–61.
6 S. Fustero, R. Román, J. F. Sanz-Cervera, A. Simón-Fuentes, A. C. Cuñat, S. Villanova and M. Murguía, *J. Org. Chem.*, 2008, **73**, 3523–3529.
7 J. Wencel-Delord and F. Colobert, *Org. Chem. Front.*, 2016, **3**, 394–400.
8 A. M. Wilders, J. Henle, M. C. Haibach, R. Swiatowiec, J. Bien, R. F. Henry, S. O. Asare, A. L. Wall and S. Shekhar, *ACS Catal.*, 2020, **10**, 15008–15018.
9 Z. Xu, Z. Hang, L. Chai and Z.-Q. Liu, *Org. Lett.*, 2016, **18**, 4662–4665.
10 B. Riniker, B. Kamber and P. Sieber, *Helv. Chim. Acta*, 1975, **58**, 1086–1094.
11 P. Sieber, B. Kamber, A. Hartmann, A. Jöhl, B. Riniker and W. Rittel, *Helv. Chim. Acta*, 1974, **57**, 2617–2621.
12 H. F. Motiwala, A. M. Armaly, J. G. Cacioppo, T. C. Coombs, K. R. K. Koehn, V. M. Norwood and J. Aube, *Chem. Rev.*, 2022, **122**, 12544–12747.
13 R. Gauthier, N. V. Tzouras, Z. Zhang, S. Bédard, M. Saab, L. Falivene, K. Van Hecke, L. Cavallo, S. P. Nolan and J. Paquin, *Chem. – Eur. J.*, 28, (4), e202103886.
14 N. V. Tzouras, A. Gobbo, N. B. Pozsoni, S. G. Chalkidis, S. Bhandary, K. Van Hecke, G. C. Vougioukalakis and S. P. Nolan, *Chem. Commun.*, 2022, **58**, 8516–8519.
15 J. Wolf, F. Huber, N. Erochok, F. Heinen, V. Guérin, C. Y. Legault, S. F. Kirsch and S. M. Huber, *Angew. Chem., Int. Ed.*, 2020, **59**, 16496–16500.
16 M. Veguillas, G. M. Rosair, M. W. P. Bebbington and A.-L. Lee, *ACS Catal.*, 2019, **9**, 2552–2557.
17 E. Jiménez-Núñez and A. M. Echavarren, *Chem. Rev.*, 2008, **108**, 3326–3350.
18 R. Ebule, S. Liang, G. B. Hammond and B. Xu, *ACS Catal.*, 2017, **7**, 6798–6801.
19 F. Nahra, N. V. Tzouras, A. Collado and S. P. Nolan, *Nat. Protoc.*, 2021, **16**, 1476–1493.
20 N. V. Tzouras, F. Nahra, L. Falivene, L. Cavallo, M. Saab, K. Van Hecke, A. Collado, C. J. Collett, A. D. Smith, C. S. J. Cazin and S. P. Nolan, *Chem. – Eur. J.*, 2020, **26**, 4515–4519.
21 E. A. Martynova, N. V. Tzouras, G. Pisano, C. S. J. Cazin and S. P. Nolan, *Chem. Commun.*, 2021, **57**, 3836–3856.
22 F. Nahra, S. R. Patrick, A. Collado and S. P. Nolan, *Polyhedron*, 2014, **84**, 59–62.
23 A. Gómez-Suárez, R. S. Ramón, A. M. Z. Slawin and S. P. Nolan, *Dalton Trans.*, 2012, **41**, 5461.
24 A. S. K. Hashmi, *Chem. Rev.*, 2021, **121**, 8309–8310.
25 B. Ranieri, I. Escofet and A. M. Echavarren, *Org. Biomol. Chem.*, 2015, **13**, 7103–7118.
26 S. Komiya, T. Sone, Y. Usui, M. Hirano and A. Fukuoka, *Gold Bull.*, 1996, **29**, 131–136.
27 Y. Usui, J. Noma, M. Hirano and S. Komiya, *Inorg. Chim. Acta*, 2000, **309**, 151–154.
28 S. Komiya, M. Iwata, T. Sone and A. Fukuoka, *J. Chem. Soc., Chem. Commun.*, 1992, 1109.
29 M. A. Cinellu and G. Minghetti, *Gold Bull.*, 2002, **35**, 11–20.
30 S. Gaillard, A. M. Z. Slawin and S. P. Nolan, *Chem. Commun.*, 2010, **46**, 2742.
31 I. I. F. Boogaerts, G. C. Fortman, M. R. L. Furst, C. S. J. Cazin and S. P. Nolan, *Angew. Chem., Int. Ed.*, 2010, **49**, 8674–8677.
32 M. Ramos, J. Poater, N. Villegas-Escobar, M. Gimferrer, A. Toro-Labbé, L. Cavallo and A. Poater, *Eur. J. Inorg. Chem.*, 2020, **2020**, 1123–1134.
33 Y. Oonishi, A. Gómez-Suárez, A. R. Martin and S. P. Nolan, *Angew. Chem., Int. Ed.*, 2013, **52**, 9767–9771.
34 N. Ibrahim, M. H. Vilhelmsen, M. Pernpointner, F. Rominger and A. S. K. Hashmi, *Organometallics*, 2013, **32**, 2576–2583.
35 S. Dupuy, L. E. Crawford, M. Bühl, A. M. Z. Slawin and S. P. Nolan, *Adv. Synth. Catal.*, 2012, **354**, 2380–2386.
36 R. D. Adams and G. Elpitiya, *Inorg. Chem.*, 2015, **54**, 8042–8048.
37 N. V. Tzouras, M. Saab, W. Janssens, T. Cauwenbergh, K. Van Hecke, F. Nahra and S. P. Nolan, *Chem. – Eur. J.*, 2020, **26**, 5541–5551.
38 T. Scattolin, N. V. Tzouras, L. Falivene, L. Cavallo and S. P. Nolan, *Dalton Trans.*, 2020, **49**, 9694–9700.
39 N. V. Tzouras, E. A. Martynova, X. Ma, T. Scattolin, B. Hupp, H. Busen, M. Saab, Z. Zhang, L. Falivene, G. Pisanò, K. Van Hecke, L. Cavallo, C. S. J. Cazin, A. Steffen and S. P. Nolan, *Chem. – Eur. J.*, 2021, **27**, 11904–11911.
40 E. A. Martynova, T. Scattolin, E. Cavarzerani, M. Peng, K. Van Hecke, F. Rizzolio and S. P. Nolan, *Dalton Trans.*, 2022, **51**, 3462–3471.
41 E. A. Martynova, V. A. Voloshkin, S. G. Guillet, F. Bru, M. Beliš, K. Van Hecke, C. S. J. Cazin and S. P. Nolan, *Chem. Sci.*, 2022, **13**, 6852–6857.
42 I. Ibni Hashim, N. V. Tzouras, W. Janssens, T. Scattolin, L. Bourda, S. Bhandary, K. Van Hecke, S. P. Nolan and C. S. J. Cazin, *Chem. – Eur. J.*, 2022, **28**(47), e202201224.
43 M. M. Hansmann, F. Rominger, M. P. Boone, D. W. Stephan and A. S. K. Hashmi, *Organometallics*, 2014, **33**, 4461–4470.

